Investigation of the topological properties of the $\mathbb{C}P^{N-1}$ model

Università di Pisa

Istituto Nazionale di Fisica Nucleare

Speaker: **Claudio Bonanno** (claudio.bonanno@pi.infn.it)

SM&FT 2017, Bari (Italy), 13 – 15 December 2017

The $\mathbb{C}P^{N-1}$ model is a 2D QFT which shares many fundamental properties with QCD such as confinement, asymptotic freedom or topological properties.

The importance of $\mathbb{C}P^{N-1}$ for NPQCD

The $\mathbb{C}P^{N-1}$ model is a 2D QFT which shares many fundamental properties with QCD such as confinement, asymptotic freedom or topological properties.

The model is analytically solvable in the non-perturbative regime in the large-N limit ($N \to \infty$). This fact helped developing the study of NPQCD (e. g. Witten, 1979).

The importance of $\mathbb{C}P^{N-1}$ for NPQCD

The $\mathbb{C}P^{N-1}$ model is a 2D QFT which shares many fundamental properties with QCD such as confinement, asymptotic freedom or topological properties.

The model is analytically solvable in the non-perturbative regime in the large-N limit ($N \to \infty$). This fact helped developing the study of NPQCD (e. g. Witten, 1979).

Besides, in recent times, the $\mathbb{C}P^{N-1}$ has been extensively studied numerically through Monte Carlo simulations:

The importance of $\mathbb{C}P^{N-1}$ for NPQCD

The $\mathbb{C}P^{N-1}$ model is a 2D QFT which shares many fundamental properties with QCD such as confinement, asymptotic freedom or topological properties.

The model is analytically solvable in the non-perturbative regime in the large-N limit ($N \to \infty$). This fact helped developing the study of NPQCD (e. g. Witten, 1979).

Besides, in recent times, the $\mathbb{C}P^{N-1}$ has been extensively studied numerically through Monte Carlo simulations:

- $\mathbb{C}P^{N-1}$ simulations need a lower numerical effort,

The importance of $\mathbb{C}P^{N-1}$ for NPQCD

The $\mathbb{C}P^{N-1}$ model is a 2D QFT which shares many fundamental properties with QCD such as confinement, asymptotic freedom or topological properties.

The model is analytically solvable in the non-perturbative regime in the large-N limit ($N \to \infty$). This fact helped developing the study of NPQCD (e. g. Witten, 1979).

Besides, in recent times, the $\mathbb{C}P^{N-1}$ has been extensively studied numerically through Monte Carlo simulations:

- $\mathbb{C}P^{N-1}$ simulations need a lower numerical effort,
- $\mathbb{C}P^{N-1}$ is the ideal test bed for new algorithms to solve QCD non-trivial computational problems,

The importance of $\mathbb{C}P^{N-1}$ for NPQCD

The $\mathbb{C}P^{N-1}$ model is a 2D QFT which shares many fundamental properties with QCD such as confinement, asymptotic freedom or topological properties.

The model is analytically solvable in the non-perturbative regime in the large-N limit ($N \to \infty$). This fact helped developing the study of NPQCD (e. g. Witten, 1979).

Besides, in recent times, the $\mathbb{C}P^{N-1}$ has been extensively studied numerically through Monte Carlo simulations:

- $\mathbb{C}P^{N-1}$ simulations need a lower numerical effort,
- $\mathbb{C}P^{N-1}$ is the ideal test bed for new algorithms to solve QCD non-trivial computational problems,
- the model offers the possibility of comparing MC results with analytic predictions.

Topology and θ-dependence

In the $\mathbb{C}P^{N-1}$ model one can introduce a topological charge Q and a corresponding θ-term in the action.

The topological term introduces a θ-dependence in the theory. It is interesting to study it for the vacuum energy density f:

$$f(\theta) \equiv -\frac{1}{V}\log Z(\theta) = \frac{1}{2}\chi\theta^2\left(1 + \sum_{n=1}^{\infty} b_{2n}\theta^{2n}\right).$$

In the $\mathbb{C}P^{N-1}$ model one can introduce a topological charge Q and a corresponding θ-term in the action.

The topological term introduces a θ-dependence in the theory. It is interesting to study it for the vacuum energy density f:

$$f(\theta) \equiv -\frac{1}{V}\log Z(\theta) = \frac{1}{2}\chi\theta^2\left(1 + \sum_{n=1}^{\infty} b_{2n}\theta^{2n}\right).$$

The θ-dependence of f is a consequence of topology:

$$\frac{d^m f}{d\theta^m} = -\frac{i^m}{V}k_m(Q) \implies \begin{cases}\chi = \langle Q^2\rangle\,|_{\theta=0}/V, \\ \chi b_2 = -\{\,\langle Q^4\rangle - \langle Q^2\rangle^2\,\}|_{\theta=0}/(12V).\end{cases}$$

The study of $f(\theta)$ is of particular relevance in QCD. Indeed, in this case:

$$\chi \sim m_{\eta'}^2 \quad \text{(E. Witten, 1979)}$$

$$b_2 \sim \eta'\text{-}\eta' \text{ elastic scattering amplitude}$$

(G. Veneziano, 1979)

The study of $f(\theta)$ is of particular relevance in QCD. Indeed, in this case:

$$\chi \sim m_{\eta'}^2 \quad \text{(E. Witten, 1979)}$$

$$b_2 \sim \eta'\text{-}\eta' \text{ elastic scattering amplitude}$$

(G. Veneziano, 1979)

Besides, $f(\theta)$ is related to axion phenomenology and, thus, to the problem of strong-CP violation.

The study of $f(\theta)$ is of particular relevance in QCD. Indeed, in this case:

$$\chi \sim m_{\eta'}^2 \quad \text{(E. Witten, 1979)}$$

$$b_2 \sim \eta'\text{-}\eta' \text{ elastic scattering amplitude}$$

(G. Veneziano, 1979)

Besides, $f(\theta)$ is related to axion phenomenology and, thus, to the problem of strong-CP violation.

In QCD, χ and b_2 cannot be computed analytically from first principles. Therefore, numerical MC simulations have been employed to this task. This motivates to perform a similar measure for the $\mathbb{C}P^{N-1}$ model.

Goals

Currently, only the topological susceptibility of the $\mathbb{C}P^{N-1}$ model has been measured numerically.

The goals of our studies are:

Goals

Currently, only the topological susceptibility of the $\mathbb{C}P^{N-1}$ model has been measured numerically.

The goals of our studies are:

- measure of the θ-dependence of the vacuum energy density $f(\theta)$ using MC simulations beyond the state of the art; in particular we aim to measure χ, b_2 and b_4,

Goals

Currently, only the topological susceptibility of the $\mathbb{C}P^{N-1}$ model has been measured numerically.

The goals of our studies are:

- measure of the θ-dependence of the vacuum energy density $f(\theta)$ using MC simulations beyond the state of the art; in particular we aim to measure χ, b_2 and b_4,
- study of their large-N limit and comparison with analytic predictions.

Sign problem

The total action is:

$$S = S_0 + S_{top} = \beta E - i\theta Q. \qquad (\beta \equiv 1/g)$$

Since $S \in \mathbb{C} \implies P \propto e^{-S}$ is not a proper probability distribution if $\theta \neq 0$.

Sign problem

The total action is:

$$S = S_0 + S_{top} = \beta E - i\theta Q. \qquad (\beta \equiv 1/g)$$

Since $S \in \mathbb{C} \implies P \propto e^{-S}$ is not a proper probability distribution if $\theta \neq 0$.

However, since we are interested in χ and in the b_{2n}, which are related to the derivatives of f evaluated at $\theta = 0$, one can limit to make simulations at $\theta = 0$.

Sign problem

The total action is:

$$S = S_0 + S_{top} = \beta E - i\theta Q. \qquad (\beta \equiv 1/g)$$

Since $S \in \mathbb{C} \implies P \propto e^{-S}$ is not a proper probability distribution if $\theta \neq 0$.

However, since we are interested in χ and in the b_{2n}, which are related to the derivatives of f evaluated at $\theta = 0$, one can limit to make simulations at $\theta = 0$.

The $\mathbb{C}P^{N-1}$ action S_0 is linear in the fields, therefore, it is easy to implement a local algorithm to sample P. For example one can use an heat-bath update.

Local algorithms, however, suffer from a serious computational problem:

Local algorithms, however, suffer from a serious computational problem:

When approaching the continuum limit ($\xi_L \to \infty$), the machine time needed to change the topological charge of a field configuration exponentially grows with ξ_L and with N.

Critical Slowing Down of Topological Modes

Local algorithms, however, suffer from a serious computational problem:

When approaching the continuum limit ($\xi_L \to \infty$), the machine time needed to change the topological charge of a field configuration exponentially grows with ξ_L and with N.

This is due to the impossibility of changing the number of windings with a local deformation in the continuum.

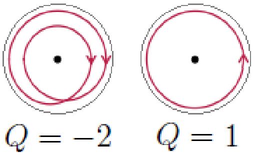

On the lattice, to change Q with a local deformation, the trajectory must pass through discontinuous configurations with divergent S in the continuum limit.

Pursued numerical strategies

In order to measure $f(\theta)$ we need to adopt numerical strategies to improve the efficiency of local MC simulations.
In particular, we chose:

Pursued numerical strategies

In order to measure $f(\theta)$ we need to adopt numerical strategies to improve the efficiency of local MC simulations.
In particular, we chose:

- simulated tempering algorithm to dampen the CSD of topological modes (Marinari and Parisi, 1992; Vicari, 1993),

Pursued numerical strategies

In order to measure $f(\theta)$ we need to adopt numerical strategies to improve the efficiency of local MC simulations.
In particular, we chose:

- simulated tempering algorithm to dampen the CSD of topological modes (Marinari and Parisi, 1992; Vicari, 1993),
- imaginary-θ method to avoid the sign problem and to improve measure accuracy of $f(\theta)$ (Panagopoulos and Vicari, 2011).

Analytic continuation

Being the θ-dependence of the theory analytic, one can continue the model for imaginary angles:

$$\theta \equiv -i\theta_I \implies S_{top} = -i\theta Q = -\theta_I Q \in \mathbb{R}.$$

Now $S \in \mathbb{R}$ and $P \propto e^{-S}$ is a proper probability distribution.

Analytic continuation

Being the θ-dependence of the theory analytic, one can continue the model for imaginary angles:

$$\theta \equiv -i\theta_I \implies S_{top} = -i\theta Q = -\theta_I Q \in \mathbb{R}.$$

Now $S \in \mathbb{R}$ and $P \propto e^{-S}$ is a proper probability distribution.

The continuation of the vacuum energy density reads:

$$f(\theta_I) = f(\theta = -i\theta_I) = -\frac{1}{2}\chi\theta_I^2 \left(1 + \sum_{n=1}^{\infty}(-1)^n b_{2n}\theta_I^{2n}\right).$$

Therefore, we can study $f(\theta_I)$ to measure χ and the b_{2n} coefficients.

Imaginary-θ fit

Now, we can measure the θ_I-dependence of the theory on the lattice. Remembering that

$$\frac{d^m f(\theta_I)}{d\theta_I^m} = -\frac{1}{V} k_m(Q)(\theta_I),$$

Now, we can measure the θ_I-dependence of the theory on the lattice. Remembering that

$$\frac{d^m f(\theta_I)}{d\theta_I^m} = -\frac{1}{V} k_m(Q)(\theta_I),$$

we can make a global fit of the θ_I-dependence of the cumulants of Q to measure χ and the b_{2n}:

$$\frac{k_1(Q)(\theta_I)}{V} = \chi\theta_I\left[1 - 2b_2\theta_I^2 + 3b_4\theta_I^4 + O(\theta_I^5)\right],$$
$$\frac{k_2(Q)(\theta_I)}{V} = \chi\left[1 - 6b_2\theta_I^2 + 15b_4\theta_I^4 + O(\theta_I^5)\right],$$
$$\frac{k_3(Q)(\theta_I)}{V} = \chi\left[- 12b_2\theta_I + 60b_4\theta_I^3 + O(\theta_I^4)\right].$$

Imaginary-θ fit

Now, we can measure the θ_I-dependence of the theory on the lattice. Remembering that

$$\frac{d^m f(\theta_I)}{d\theta_I^m} = -\frac{1}{V} k_m(Q)(\theta_I),$$

we can make a global fit of the θ_I-dependence of the cumulants of Q to measure χ and the b_{2n}:

$$\frac{k_1(Q)(\theta_I)}{V} = \chi\theta_I\big[1 - 2b_2\theta_I^2 + 3b_4\theta_I^4 + O(\theta_I^5)\big],$$
$$\frac{k_2(Q)(\theta_I)}{V} = \chi\big[1 - 6b_2\theta_I^2 + 15b_4\theta_I^4 + O(\theta_I^5)\big],$$
$$\frac{k_3(Q)(\theta_I)}{V} = \chi\big[- 12b_2\theta_I + 60b_4\theta_I^3 + O(\theta_I^4)\big].$$

On the lattice: $\theta_I = Z_\theta \theta_L$.

The simulated tempering consists in promoting the temperature T as a dynamical variable.

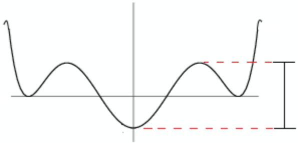

The systems heats up during its evolution and can escape from the local minima in which it is trapped.

The simulated tempering algorithm

The simulated tempering consists in promoting the temperature T as a dynamical variable.

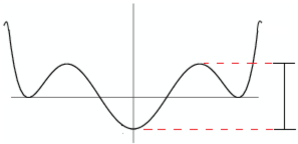

The systems heats up during its evolution and can escape from the local minima in which it is trapped.

In the case of the $\mathbb{C}P^{N-1}$ model, we promoted both β and θ_I to dynamical variables:

$$P \propto e^{-S} = e^{-\beta E + \theta_I Q}.$$

The simulated tempering algorithm

The simulated tempering consists in promoting the temperature T as a dynamical variable.

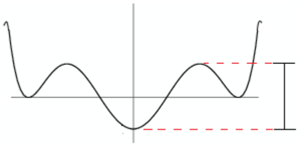

The systems heats up during its evolution and can escape from the local minima in which it is trapped.

In the case of the $\mathbb{C}P^{N-1}$ model, we promoted both β and θ_I to dynamical variables:

$$P \propto e^{-S} = e^{-\beta E + \theta_I Q}.$$

- When β decreases, the height of the topological barriers decreases too and the algorithm changes Q more easily.

The simulated tempering consists in promoting the temperature T as a dynamical variable.

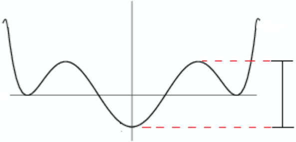

The systems heats up during its evolution and can escape from the local minima in which it is trapped.

In the case of the $\mathbb{C}P^{N-1}$ model, we promoted both β and θ_I to dynamical variables:

$$P \propto e^{-S} = e^{-\beta E + \theta_I Q}.$$

- When β decreases, the height of the topological barriers decreases too and the algorithm changes Q more easily.
- When θ_I increases, higher-charge configurations are more probable to realize. Indeed, $\langle Q \rangle$ is an increasing function of θ_I.

Simulated tempering set-up

The simulated tempering requires a quite complex set-up, in particular when choosing the allowed values of β.

Simulated tempering set-up

The simulated tempering requires a quite complex set-up, in particular when choosing the allowed values of β.

- $\beta_{min} \to$ local algorithm decorrelates fast,

Simulated tempering set-up

The simulated tempering requires a quite complex set-up, in particular when choosing the allowed values of β.

- $\beta_{min} \to$ local algorithm decorrelates fast,
- $\beta_{max} \to$ how close one wants to get to the continuum limit,

Simulated tempering set-up

The simulated tempering requires a quite complex set-up, in particular when choosing the allowed values of β.

- $\beta_{min} \to$ local algorithm decorrelates fast,
- $\beta_{max} \to$ how close one wants to get to the continuum limit,
- $\delta\beta_i \to$ reasonable acceptance of change of β.

Simulated tempering set-up

The simulated tempering requires a quite complex set-up, in particular when choosing the allowed values of β.

- $\beta_{min} \rightarrow$ local algorithm decorrelates fast,
- $\beta_{max} \rightarrow$ how close one wants to get to the continuum limit,
- $\delta\beta_i \rightarrow$ reasonable acceptance of change of β.

The correct choice of $\delta\beta_i$ is obtained when there is a reasonable overlap between the probability distributions of the energy at different temperatures.

Simulated tempering set-up

The simulated tempering requires a quite complex set-up, in particular when choosing the allowed values of β.

- $\beta_{min} \rightarrow$ local algorithm decorrelates fast,
- $\beta_{max} \rightarrow$ how close one wants to get to the continuum limit,
- $\delta\beta_i \rightarrow$ reasonable acceptance of change of β.

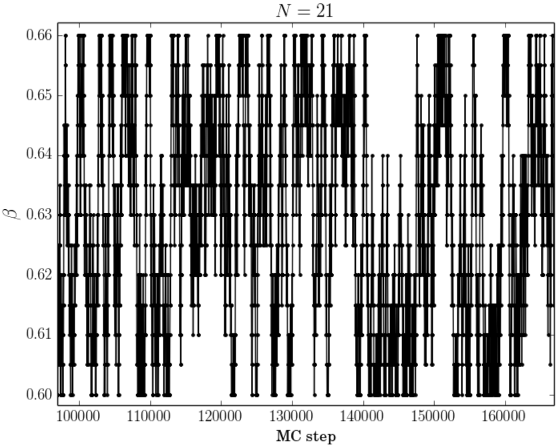

The correct choice of $\delta\beta_i$ is obtained when there is a reasonable overlap between the probability distributions of the energy at different temperatures.

Results obtained with the imaginary-θ fit

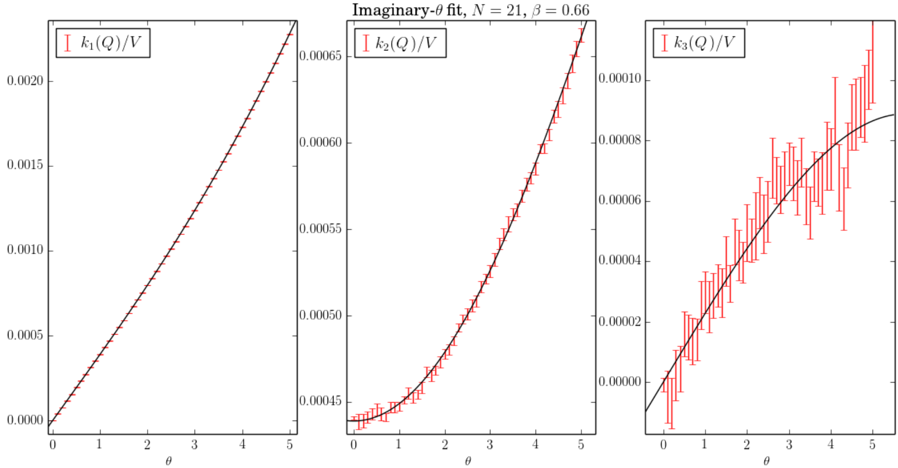

$\mathcal{O}(\beta = 0.66, N = 21)$	Standard method	Imaginary-θ	Gain
$\chi \cdot 10^4$	4.401(11)	4.3908(58)	~ 2
$b_2 \cdot 10^3$	$-5.36(40)$	$-4.958(76)$	~ 5
$b_4 \cdot 10^5$	-11 ± 21	$-1.27(20)$	~ 100

Monte Carlo evolution of Q with simulated tempering

The simulated tempering allows to dampen the freezing of the MC evolution of the topological charge.

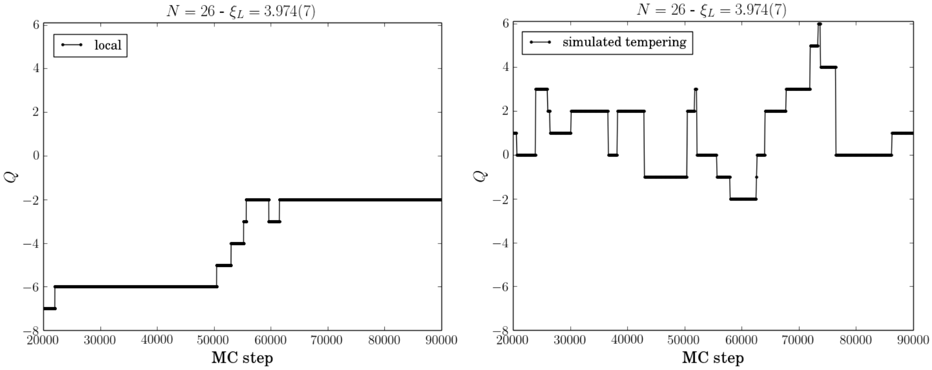

Large-N limit of topological susceptibility

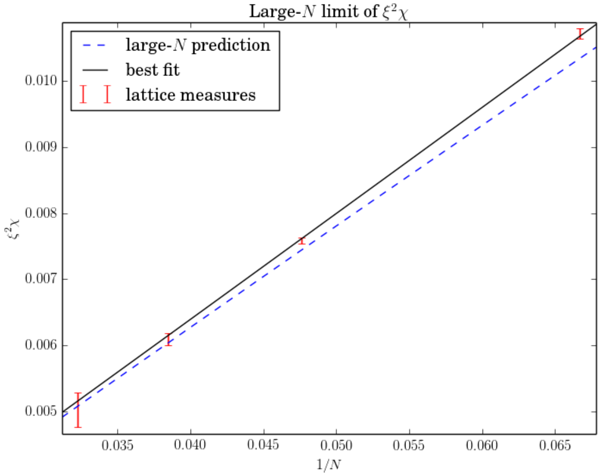

The next-to-leading term is at odds with the analytic prediction. (Campostrini and Rossi, 1991)

$$(\xi^2\chi)_{theo} = 0.1591549\frac{1}{N} - 0.0606\frac{1}{N^2}$$

$$(\xi^2\chi)_{fit} = 0.1591(4)\frac{1}{N} + 0.015(9)\frac{1}{N^2}$$

Large-N limit of b_2 and b_4

Corrections to the leading behaviour predicted by analytic calculations (Bonati, D'Elia, Rossi and Vicari, 2016) are still large in the explored range of N for the b_{2n} coefficients.

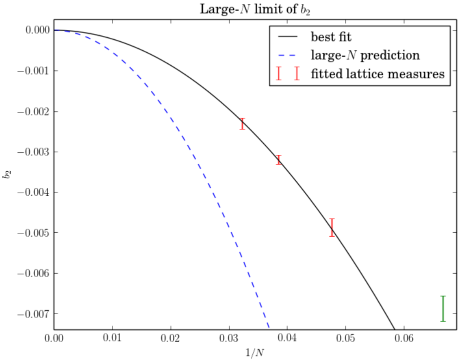

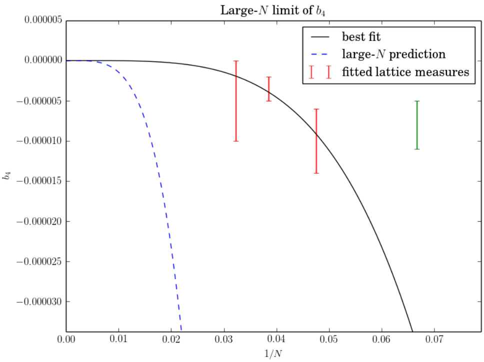

Summary and future perspective

Summarizing, our work consisted in:

Summary and future perspective

Summarizing, our work consisted in:

- application of the imaginary-θ method and of the simulated tempering algorithm to the $\mathbb{C}P^{N-1}$ model to improve the efficiency of simulations,

Summary and future perspective

Summarizing, our work consisted in:

- application of the imaginary-θ method and of the simulated tempering algorithm to the $\mathbb{C}P^{N-1}$ model to improve the efficiency of simulations,
- lattice measures of χ, b_2 and b_4 and improvement of the state of the art about the knowledge of $f(\theta)$,

Summary and future perspective

Summarizing, our work consisted in:

- application of the imaginary-θ method and of the simulated tempering algorithm to the $\mathbb{C}P^{N-1}$ model to improve the efficiency of simulations,
- lattice measures of χ, b_2 and b_4 and improvement of the state of the art about the knowledge of $f(\theta)$,
- numerical study of the large-N limit of χ, b_2 and b_4 and comparison with theoretical predictions.

Summary and future perspective

Summarizing, our work consisted in:

- application of the imaginary-θ method and of the simulated tempering algorithm to the $\mathbb{C}P^{N-1}$ model to improve the efficiency of simulations,
- lattice measures of χ, b_2 and b_4 and improvement of the state of the art about the knowledge of $f(\theta)$,
- numerical study of the large-N limit of χ, b_2 and b_4 and comparison with theoretical predictions.

In the next future we plan to:

Summary and future perspective

Summarizing, our work consisted in:

- application of the imaginary-θ method and of the simulated tempering algorithm to the $\mathbb{C}P^{N-1}$ model to improve the efficiency of simulations,
- lattice measures of χ, b_2 and b_4 and improvement of the state of the art about the knowledge of $f(\theta)$,
- numerical study of the large-N limit of χ, b_2 and b_4 and comparison with theoretical predictions.

In the next future we plan to:

- refine measures of b_4,

Summary and future perspective

Summarizing, our work consisted in:

- application of the imaginary-θ method and of the simulated tempering algorithm to the $\mathbb{C}P^{N-1}$ model to improve the efficiency of simulations,
- lattice measures of χ, b_2 and b_4 and improvement of the state of the art about the knowledge of $f(\theta)$,
- numerical study of the large-N limit of χ, b_2 and b_4 and comparison with theoretical predictions.

In the next future we plan to:

- refine measures of b_4,
- include larger and smaller N in our analysis to improve the study of the large-N limit.

Summary and future perspective

Summarizing, our work consisted in:

- application of the imaginary-θ method and of the simulated tempering algorithm to the $\mathbb{C}P^{N-1}$ model to improve the efficiency of simulations,
- lattice measures of χ, b_2 and b_4 and improvement of the state of the art about the knowledge of $f(\theta)$,
- numerical study of the large-N limit of χ, b_2 and b_4 and comparison with theoretical predictions.

In the next future we plan to:

- refine measures of b_4,
- include larger and smaller N in our analysis to improve the study of the large-N limit.
- apply the simulated tempering on β to lattice QCD.

Thank you for your attention!

Continuum action

The continuum Euclidean action of the model we chose is:

$$S_0 = \frac{N}{g_0} \int d^2x \, \bar{D}_\mu \bar{z} D_\mu z,$$

where D_μ is the covariant derivative: $D_\mu = \partial_\mu + iA_\mu$.

The field A_μ is not propagating but it is useful to consider it independent from z.

Usually, the following parametrization is used:

$$\beta \equiv \frac{1}{g_0}, \quad E \equiv g_0 S_0 \implies S_0 = \beta E.$$

Lattice action

The discretized action we chose is:

$$S_0^{(L)} = -\frac{8}{3} N\beta \sum_{x\in Lat} \sum_{\mu=1}^{2} \Re[\bar{U}_\mu(x)\bar{z}(x+\hat{\mu})z(x)]$$

$$+\frac{1}{6} N\beta \sum_{x\in Lat} \sum_{\mu=1}^{2} \Re[\bar{U}_\mu(x+\hat{\mu})\bar{U}_\mu(x)\bar{z}(x+2\hat{\mu})z(x)].$$

$$z(x) \xleftarrow{U_\mu(x)} z(x+\hat{\mu}) \qquad U_\mu(x) \sim \exp\{iaA_\mu(x)\}$$

The topological charge definition we adopted is expressed through the magnetic flux:

$$Q = \frac{1}{2\pi} \oint_{S^1(\infty)} A_\mu \, dx_\mu = \frac{1}{2\pi} \Phi(B) = n \in \mathbb{Z}.$$

There are several possible discretization of Q:

- $Q_L = \dfrac{1}{4\pi} \displaystyle\sum_{x \in Lat} \sum_{\mu,\nu=1}^{2} \Im\{ i\varepsilon_{\mu\nu} \Pi_{\mu\nu}(x) \},$ (Non-geometric)
- $Q_U = \dfrac{1}{2\pi} \displaystyle\sum_{x \in Lat} \Im \left[\log \left(\Pi_{12}(x) \right) \right],$ (Geometric)

where $\Pi_{\mu\nu}$ is the plaquette operator:

$$\Pi_{\mu\nu}(x) \equiv U_\mu(x) U_\nu(x+\hat{\mu}) \bar{U}_\mu(x+\hat{\nu}) \bar{U}_\nu(x).$$

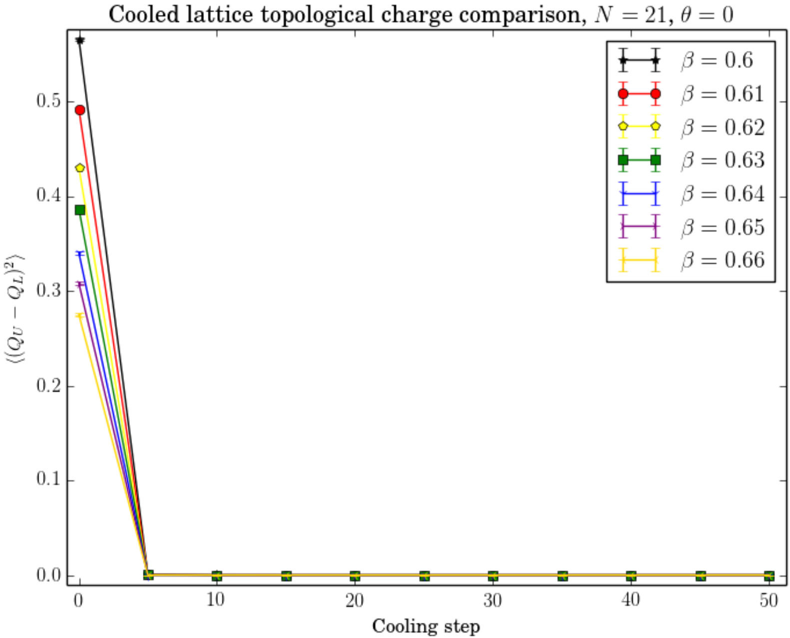
Cooled lattice topological charge comparison, $N = 21$, $\theta = 0$
$\langle (Q_U - Q_L)^2 \rangle$
Cooling step
$\beta = 0.6$
$\beta = 0.61$
$\beta = 0.62$
$\beta = 0.63$
$\beta = 0.64$
$\beta = 0.65$
$\beta = 0.66$
0.0
0.1
0.2
0.3
0.4
0.5
0
10
20
30
40
50

Topological Charge Freezing

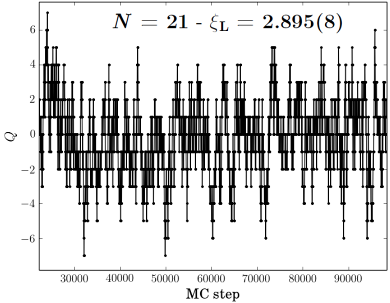

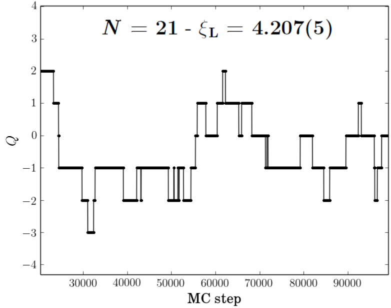

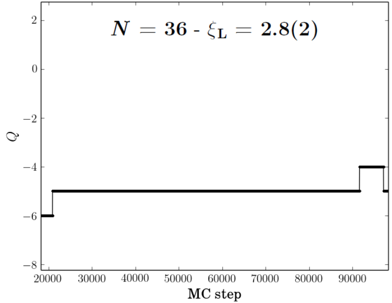

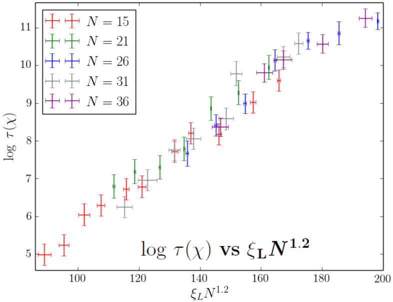

Metropolis acceptance of β change:

$$p \approx \exp\left\{\delta\beta(\bar{U} - E)\right\}, \quad \bar{U} = [U(\beta_{new}) - U(\beta_{old})]/2$$

$$\Longrightarrow \; p = O(1) \iff \bar{U} \approx E \iff E \in \text{ overlap region}$$

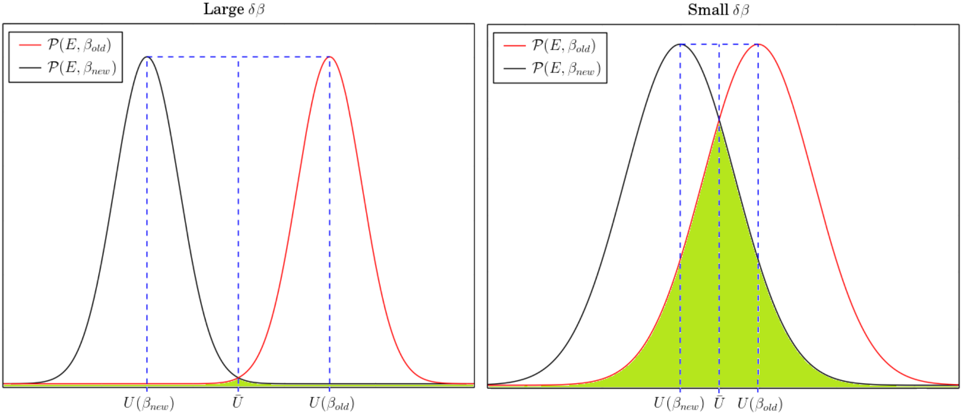

Determination of the free energy

A rough estimation of the free energy is needed to avoid non-ergodicity:

$$P \propto e^{-\beta E+\theta_I Q_L+F(\beta,\theta_I)}$$

To estimate $F(\beta, \theta_I)$ one can use these two relations:

- $\dfrac{\partial F}{\partial \beta} = \langle E \rangle$
- $\dfrac{\partial F}{\partial \theta_I} = -\langle Q_L \rangle$

Both $\langle E \rangle$ and $\langle Q_L \rangle$ can be easily measured in a MC simulation. Then, with a numerical integration, one can obtain F.

Simulated tempering set-up example

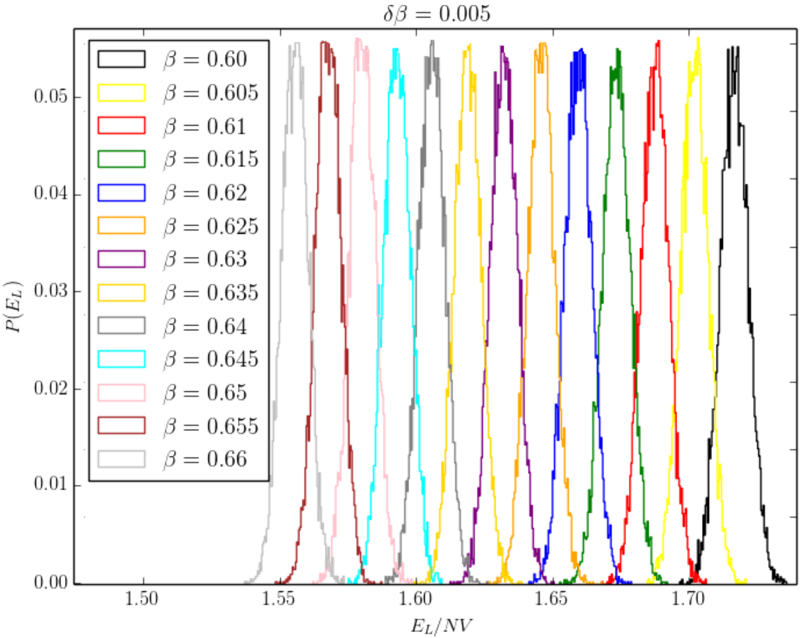

MC θ evolution with simulated tempering

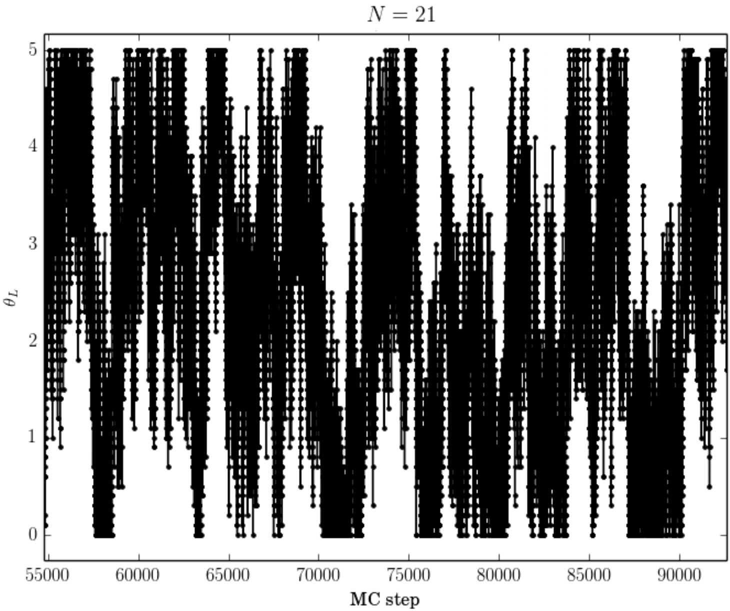

Gain achieved with the simulated tempering

The gain achieved with the simulated tempering can be expressed as:

$$G = \frac{\tau_{local}(\chi)}{\tau_{simul.\ temp.}(\chi)}.$$

where τ is the autocorrelation time at equal CPU time.

N	$\max \xi_L$	$\tau_{local}(\chi) \cdot 10^{-3}$	$\tau_{simul.\ temp.}(\chi) \cdot 10^{-3}$	G
21	4.207(5)	20.9(2.6)	10.56(62)	~ 2
26	3.974(7)	61.0(9.0)	15.64(67)	~ 4

The actual gain is $> G$ since we used all the intermediate values of θ and β generated. However, the simulated tempering introduces correlations, thus, it is not simple to estimate quantitatively the actual gain. (work in progress)

β-correlations introduced by simulated tempering

$$C(\delta\beta) \equiv \frac{Cov[Q(\beta_{max}), Q(\beta_{max} - \delta\beta)]}{\sqrt{Var[Q(\beta_{max})]\, Var[Q(\beta_{max} - \delta\beta)]}}$$

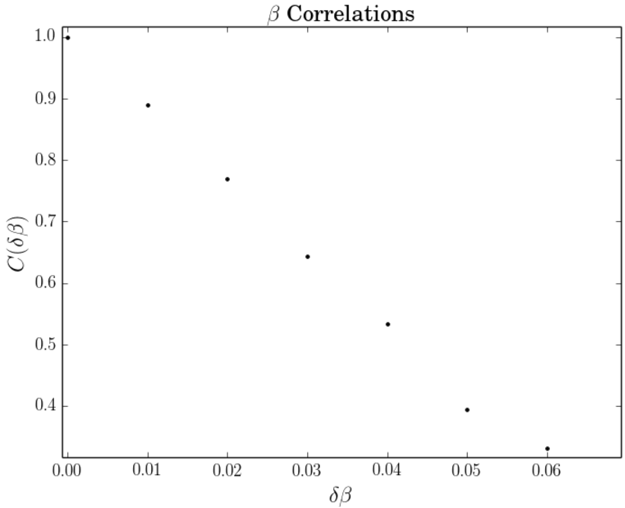

θ-correlations introduced by simulated tempering

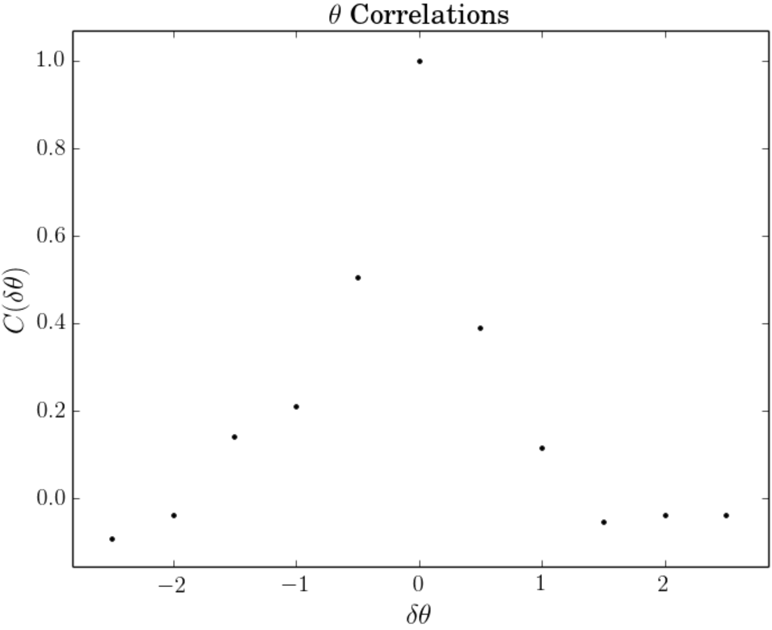

Continuum limit of $\xi^2\chi$

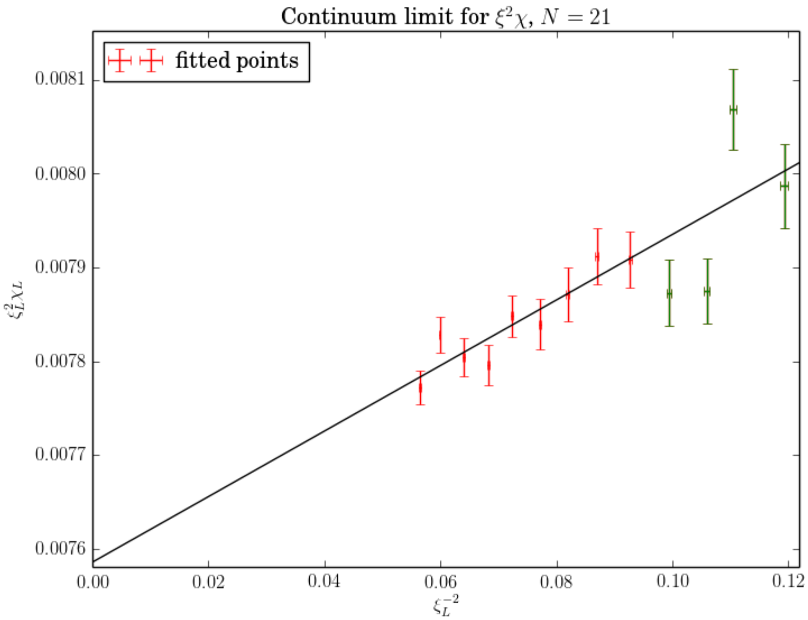

Continuum limit of b_2

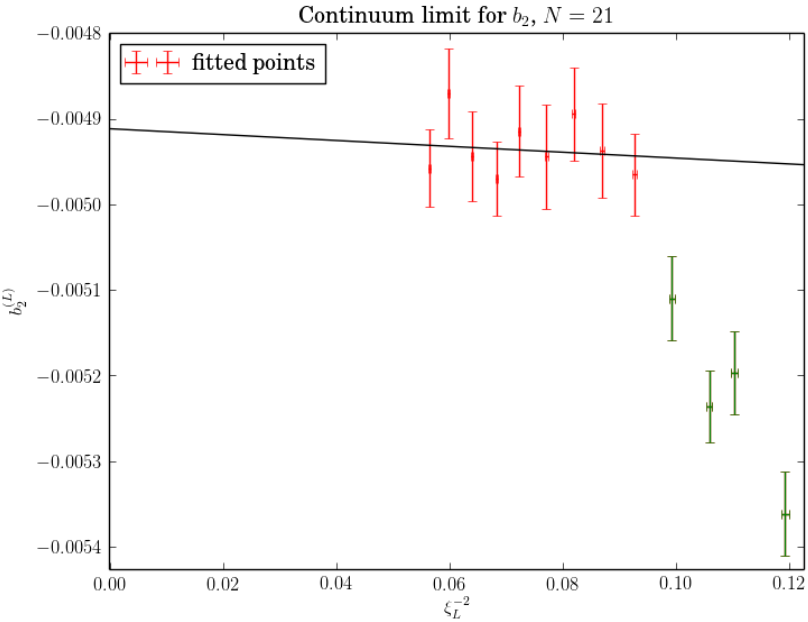

Continuum limit of b_4

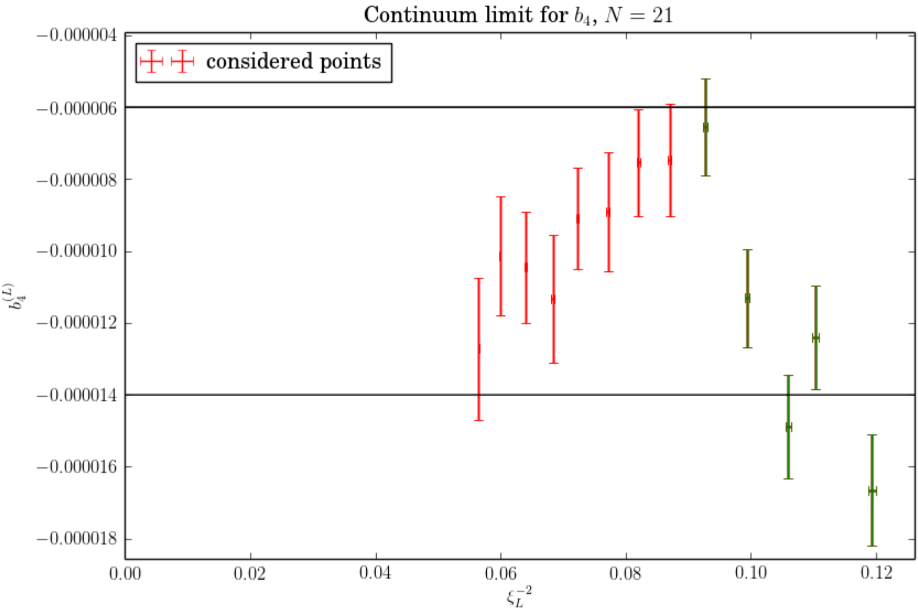

The topological susceptibility of the $\mathbb{C}P^{N-1}$ model has been extensively studied in literature. We compared our results for $N = 21$ with previous determinations.

	$\xi^2\chi(N = 21) \cdot 10^4$
Vicari, 1993	76(3)
Del Debbio, Manca and Vicari, 2004	80(2)
Hasenbusch, 2017	76.7(5)
This work, 2017	75.9(6)

The agreement between our results and the one obtained by Hasenbusch is non-trivial since, in his work, $\xi^2\chi$ was measured starting from a different discretized action.

Over-heat-bath update

The path sampling is achieved through a local over-heat-bath update of the field configuration, performed site by site. Locally, indeed, one has:

$$E(x) = \Re\{\bar{F}(x)z(x)\} = (\,F(x), z(x)\,)_N = |F|_N \cos\alpha$$

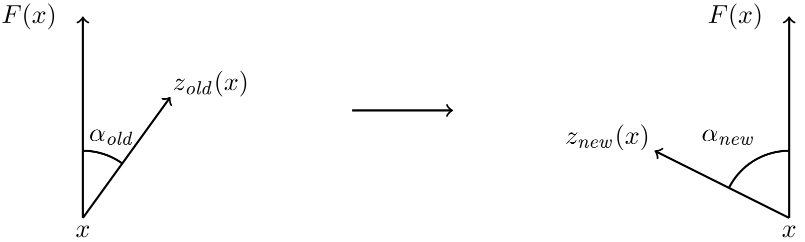

Before the update. After the update.

We ran a $C{+}{+}$ implementation of this algorithm on the computing resources of INFN - Pisa for about $6 \cdot 10^5$ core-hours.

Continuum limit

The continuum limit is achieved when $a \to 0$, id est when the lattice tends to a continuum space-time.
Practically, this limit is achieved by virtue of asymptotic freedom:

$$a \to 0 \implies \Lambda_{UV} = 1/a \to \infty,$$

$$g_0 \to 0 \implies \beta \to \infty$$

In this limit, the dimensionless correlation length of the lattice theory diverges as $1/a$: $\xi_{lattice} \sim \xi_{continuum}/a$. Thus:

$$\langle \mathcal{O} \rangle_{lattice} = \langle \mathcal{O} \rangle_{continuum} + ca + \ldots$$

$$\to \langle \mathcal{O} \rangle_{lattice} = \langle \mathcal{O} \rangle_{continuum} + c\xi_{lattice}^{-1} + \ldots$$

Quantization of the topological charge

The request of having finite action is satisfied if $z(x)$ and $A_\mu(x)$ approach, for $|x| \to \infty$, pure gauge configurations:

$$z(x) \underset{|x|\to\infty}{\sim} e^{-i\Lambda(x)} v, \quad A_\mu(x) \underset{|x|\to\infty}{\sim} \partial_\mu \Lambda(x)$$

Thus, the topological charge measures the variation of the phase Λ on a large circle:

$$2\pi Q = \oint_{S^1(\infty)} \partial_\mu \Lambda \, dx_\mu$$

Since z is a regular, single-valued function, this variation must be an integer multiple of $2\pi \implies Q = n \in \mathbb{Z}$.

Monte Carlo simulations are based on the lattice regularization of the path integral

$$\langle 0|\, \mathcal{O}\, |0\rangle \equiv \langle \mathcal{O} \rangle = \frac{\int [d\bar{z}\, dz\, dA] e^{-S[\bar{z},z,A]} \mathcal{O}[\bar{z}, z, A]}{\int [d\bar{z}\, dz\, dA] e^{-S[\bar{z},z,A]}}.$$

This regularization is achieved replacing continuum space-time with a finite-size lattice:

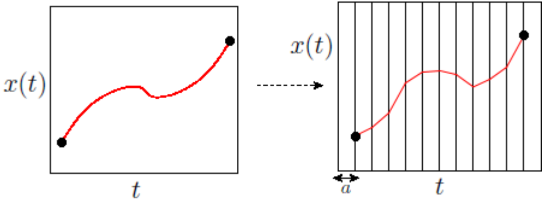

MC simulations consist in sampling the path integral and in estimating $\langle \mathcal{O} \rangle$ on the collected sample:

$$P \propto e^{-S} \implies \langle \mathcal{O} \rangle \to \langle \mathcal{O} \rangle_{lattice} = \frac{1}{n} \sum_i \mathcal{O}_i.$$